

## **Double Polymer Sheathed Carbon Nanotube Supercapacitors Show Enhanced Cycling Stability**

Wenqi Zhao,<sup>1</sup> Shanshan Wang,<sup>2</sup> Chunhui Wang,<sup>1</sup> Shiting Wu,<sup>3</sup> Wenjing Xu,<sup>3</sup> Mingchu Zou,<sup>3</sup>  
An Ouyang,<sup>3</sup> Anyuan Cao,<sup>3\*</sup> Yibin Li<sup>1\*</sup>

<sup>1</sup> Centre for Composite Materials and Structures, Harbin Institute of Technology, Harbin 150080, P. R. China

<sup>2</sup> School of Marine Science and Technology, Harbin Institute of Technology at Weihai, Weihai 264209, P. R. China

<sup>3</sup> Department of Materials Science and Engineering, College of Engineering, Peking University, Beijing 100871, P. R. China

\*Corresponding authors: Email: [liyibin@hit.edu.cn](mailto:liyibin@hit.edu.cn), [anyuan@pku.edu.cn](mailto:anyuan@pku.edu.cn)

### **Supporting Information:**

**Figure S1. Lower and higher magnification SEM images of (a, d) CNT sponges, (b, e) CNT/PANI sponges and (c, f) CNT/PPy/PANI sponges, respectively.**

**Figure S2. Cross-sectional SEM images of a double-sheath sponge (CNT/PANI/PPy) with reversed polymer coating sequence. Inset in (a): photos of a CNT/PANI/PPy sponge which can be bent or rolled up.**

**Figure S3. TEM images of the nanotubes or core-shell structures dispersed from the original CNT sponge, the CNT/PANI sponge, and the final CNT/PANI/PPy sponge.**

**Figure S4. XRD patterns of the CNT, CNT/PANI and CNT/PPy/PANI sponges, respectively.**

**Figure S5. Raman spectra of the original CNT sponge and the single-sheathed CNT/PANI sponge, and the CNT sponge and the double-sheathed CNT/PPy/PANI sponge.**

**Figure S6. Relationship between the deposition time of PANI on a CNT/PPy sponge and the electrochemical behavior of the resulting CNT/PPy/PANI sponge, showing a continuous increase of specific capacitance and then saturation for longer deposition period.**

**Figure S7. Capacitance retention recorded during cycling tests on a CNT/PANI/PPy sponge over 20000 CV cycles at a scan rate of 200 mV/s.**

**Figure S8. SEM images of CNT/PANI sponges and CNT/PPy/PANI sponges after 1000 CV cycles.**

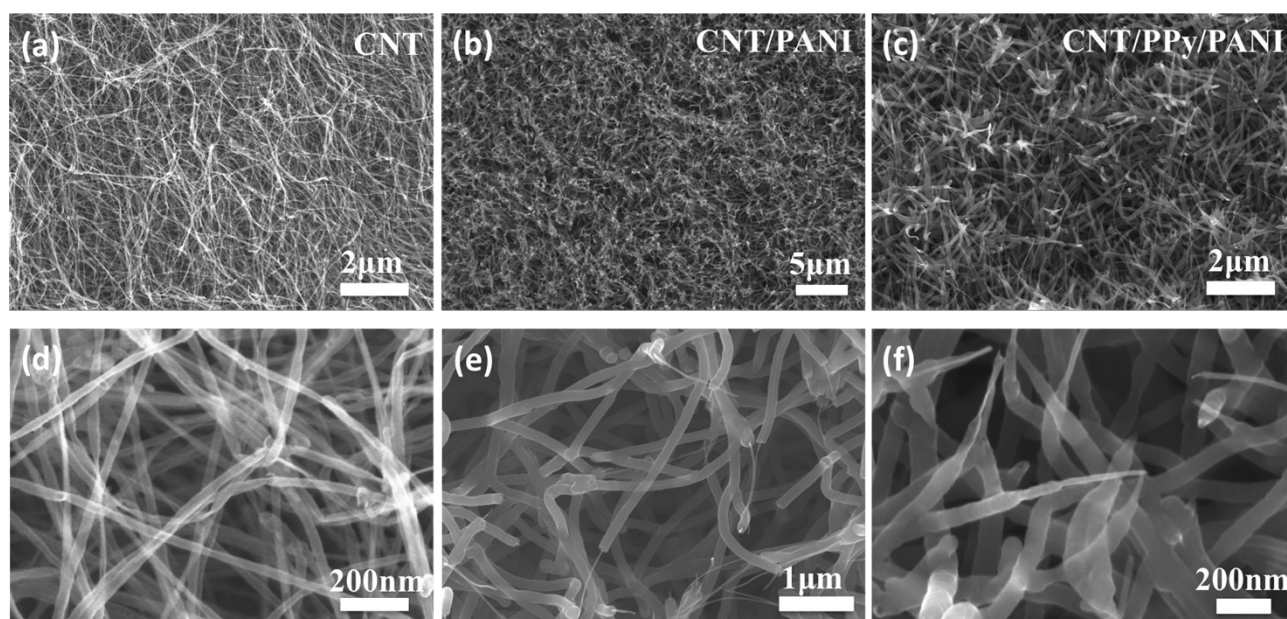


**Figure S1. Lower and higher magnification SEM images of (a, d) CNT sponges, (b, e) CNT/PANI sponges and (c, f) CNT/PPy/PANI sponges, respectively.**

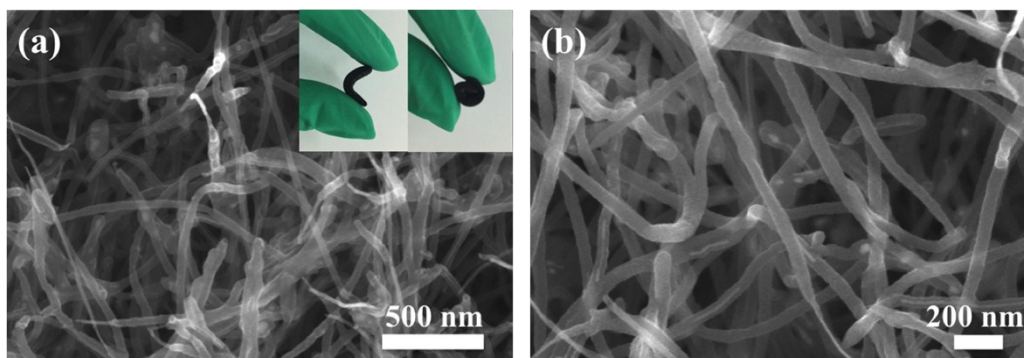


**Figure S2. Cross-sectional SEM images of a double-sheath sponge (CNT/PANI/PPy) with reversed polymer coating sequence. Inset in (a): photos of a CNT/PANI/PPy sponge which can be bent or rolled up.**

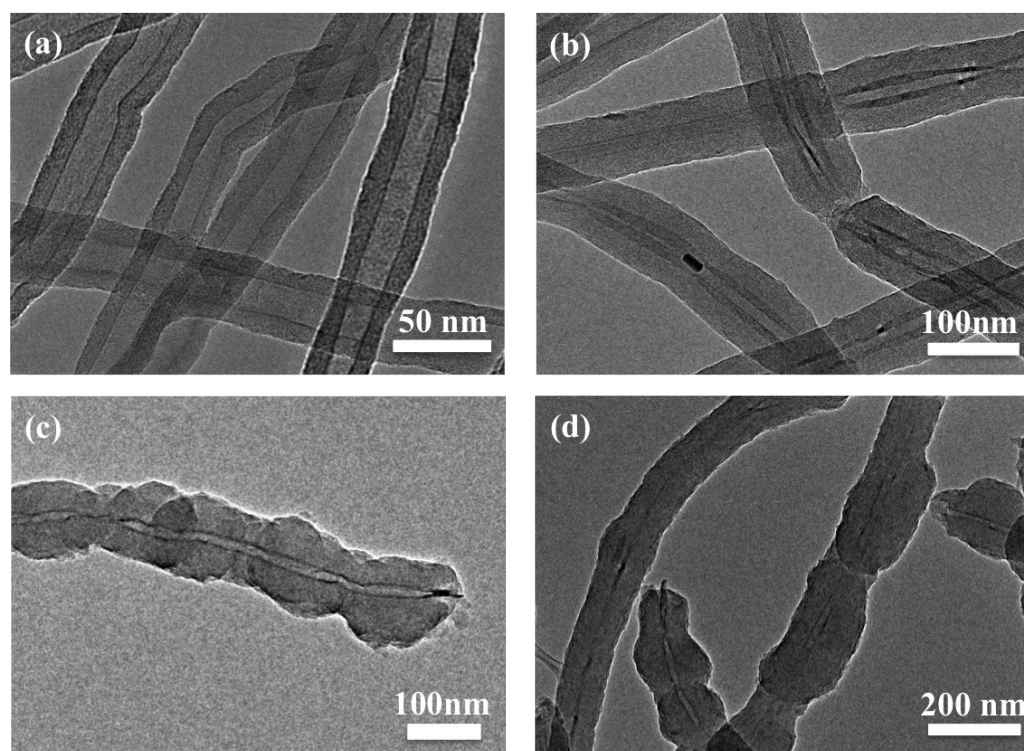


**Figure S3. TEM images of the nanotubes or core-shell structures dispersed from (a) the original CNT sponge, (b) the CNT/PANI sponge, and (c, d) the final CNT/PANI/PPy sponge.**

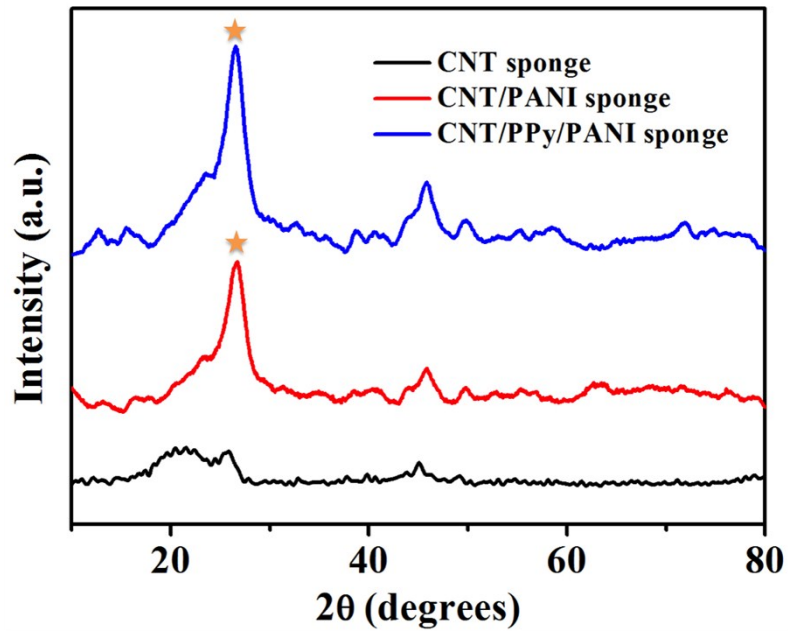


Figure S4. XRD patterns of the CNT, CNT/PANI and CNT/PPy/PANI sponges, respectively.

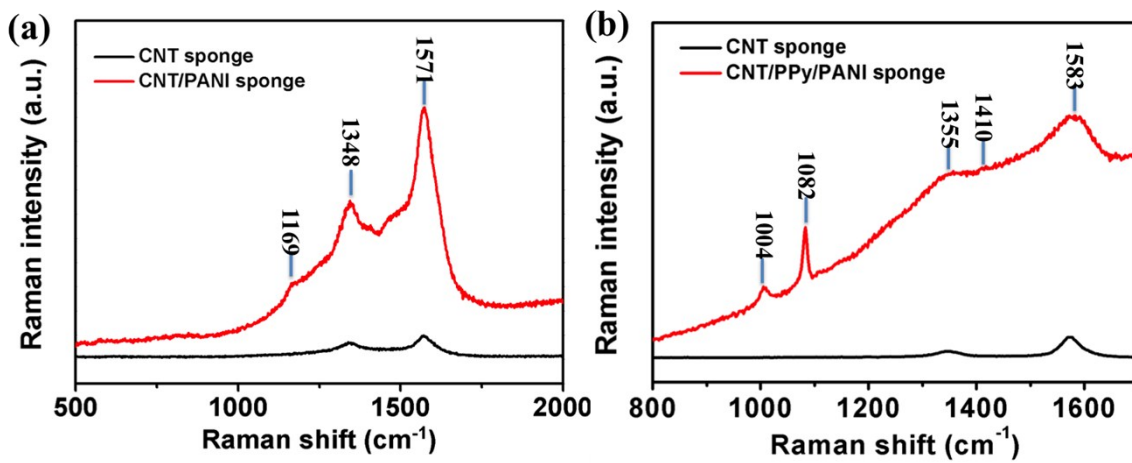


Figure S5. Raman spectra of (a) the original CNT sponge and the single-sheathed CNT/PANI sponge, and (b) the CNT sponge and the double-sheathed CNT/PPy/PANI sponge.

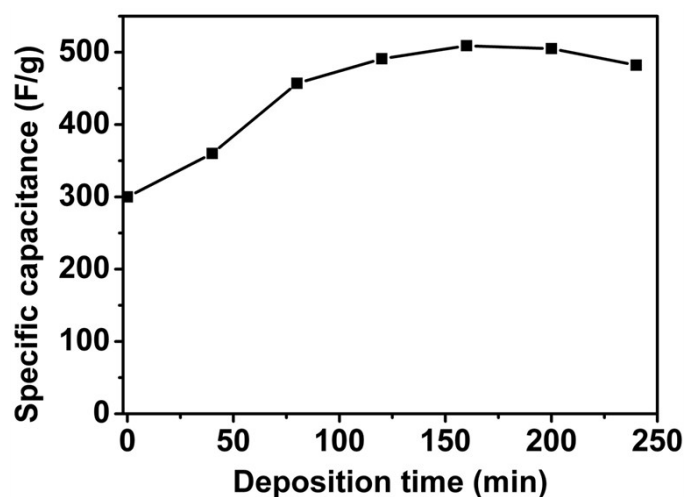


Figure S6. Relationship between the deposition time of PANI on a CNT/PPy sponge and the electrochemical behavior of the resulting CNT/PPy/PANI sponge, showing a continuous increase of specific capacitance and then saturation for longer deposition period.

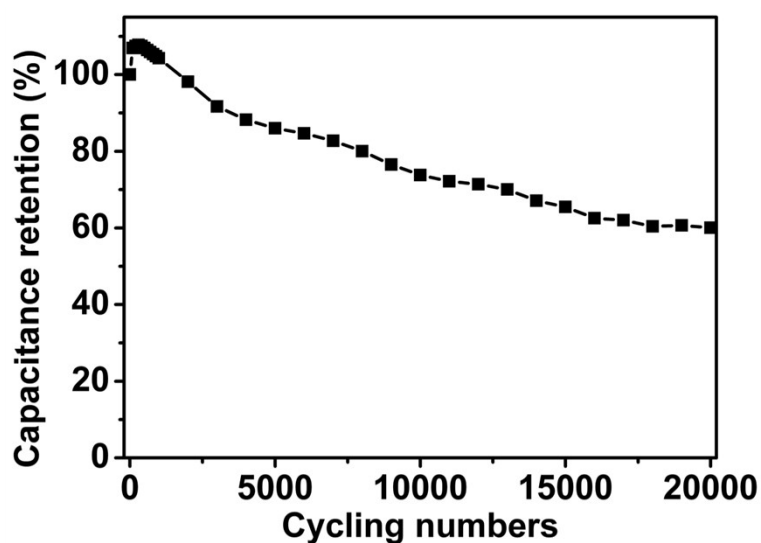
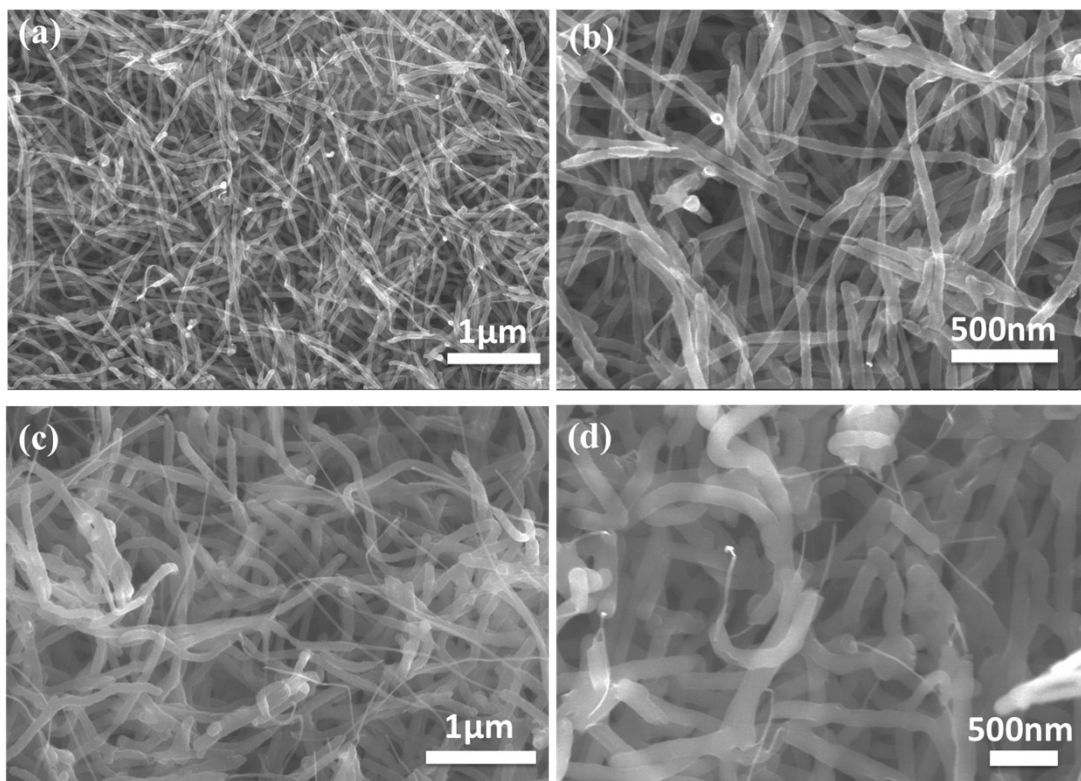


Figure S7. Capacitance retention recorded during cycling tests on a CNT/PANI/PPy sponge over 20000 CV cycles at a scan rate of 200 mV/s.



**Figure S8. SEM images of (a), (b) CNT/PANI sponges and (c), (d) CNT/PPy/PANI sponges after 1000 CV cycles.**